Design of S690 Slender Plate I-Girders under combined Shear, Bending and Compression

Henrique Gonçalves Afonso

Abstract

This work presents the design of S690 high-strength steel plate girder beams, with welded sections and longitudinal stiffeners, subjected to combined N-M-V internal forces, as is usually the case of steel beams used in steel and composite steel-concrete bridge decks. The ultimate strength of this type of slender beams is evaluated by adopting the formulation proposed in the EN 1993-1-5 standard and the recently proposed formulation by Biscaya [1] for steel plate girders. A parametric study is carried out comparing the results obtained by these formulations with the results obtained by physically and geometrically nonlinear finite element models (GMNIA). Based on this study, it is shown that the new N-M-V interaction equations proposed by Biscaya give better results in relation to those obtained by the current EN 1993-1-5 formulation, both for HSS 690 plate girder beams with longitudinal stiffeners.

Keywords: N-M-V interaction, EN 1993-1-5, high strength steel S690, slender plate girder, longitudinal stiffeners, cable stayed bridges.

1. Introduction

1.1. Overview

Slender plate girders strengthened with transverse and longitudinal stiffeners have been increasingly used in the design of cable-stayed bridges in the past few years. Besides being an economical solution, it allows the construction of bridges with medium to long spans, something that is important nowadays. However, the design of this structures may become a challenge to the most designers, once the cable-stayed bridge decks, supported by the slender plate I-girders, are subjected to high compression forces, apart from bending and shear that are commonly present in those structures. Thus, to ensure the safety of these steel I-girders, N-M-V interaction should be checked. Though, it has been proven that the formulations present in the current version of EN 1993-1-5 [2] does not give the best assessment of the real interaction of the forces. In that regard, it is worth noting the investigations conducted by Sinur and Beg [3, 4], and Jáger and Kövesdi [5, 6], who have numerically and experimentally studied the bending-shear interaction (M-V interaction) without compression for a large range of stiffened and unstiffened I-girders. Recently, Biscaya [7] studied the behaviour of unstiffened I-girders to the interaction of N-M-V stresses, developing expressions that proven to give better results than the current formulation given by EN 1993-1-5. Thus, in partnership with studies for common resistance steels (S355), one of the main goals of this study is to verify if the formulation developed for slender plate girders can be extended to longitudinally stiffened I-girders for high strength steels (S690). If not, improvements will be given to obtain a general method of calculation. Finally, it will be possible to compare the new Biscaya proposal for the N-M-V interaction stresses with the standard formulations.

1.2. N-M-V interaction following the EN 1993-1-5

Following the EN 1993-1-5 [2] principles, considering the effective width method (EWM), the design verification of slender steel plate I-girders to the N-M-V interaction is checked by the next equations, depending on the compression level of the web. Neglecting the eccentricity due to local web bucking, e_N, the relations between the applied and resistance forces are defined by $\eta_1 = \frac{M_{Ed}}{M_{eff.Rd}}$, $\bar{\eta}_3 = \frac{V_{Ed}}{V_{bw.Rd}}$ and $\eta_4 = \frac{N_{Ed}}{N_{eff.Rd}}$, ensuring that those values are always lower or equal to the unit. According to the current European standard, the N-M-V surface has two different resistance levels, depending on whether the web is fully compressed or not (Figure 1), which is not believed to make sense once it does not form a continuous surface of resistance to the N-M-V interaction. Approximately to 45º with the N-M plane, there is clearly a mismatch of the resistance surface. In fact, this can lead to uncertainties since it becomes unclear how to design these elements in the vicinity of this discontinuity.

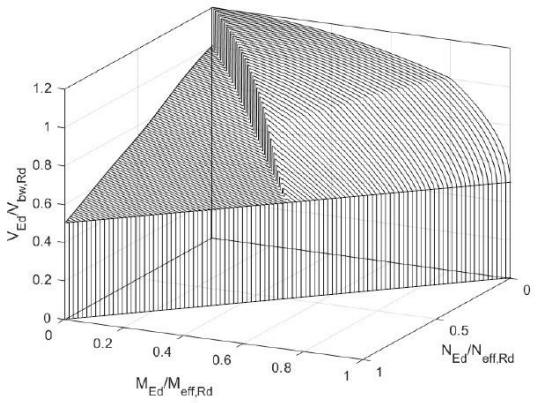

Figure 1: N-M-V interaction diagram given in EN 1993-1-5 [7]

$$\eta_1 + \eta_4 + (1 - \eta_{1.f}).(2\bar{\eta}_3 - 1)^{\mu} = 1 \qquad , \eta_1 \geq \eta_{1.f} \qquad (1)$$

$$\bar{\eta}_3 = \bar{\eta}_3^{máx} + \frac{V_{bf.Rd}}{V_{bw.Rd}}.\left\{1 - \left[\frac{M_{Ed}}{M_{f.Rd}.\left(1 - \frac{N_{Ed}}{2.N_{f.Rd}}\right)}\right]^2\right\} \qquad , \eta_1 < \eta_{1.f} \qquad (2)$$

where $\bar{\eta}_3^{máx}$ is the maximum value of $\bar{\eta}_3$ obtained accordingly to Eq. 1, and $N_{f.Rd}$ is the ultimate compressive resistance of a single flange, hence it is always multiplied by the factor 2.

$$\begin{aligned} &\eta_{1.f} = \frac{M_{f.Rd}(1 - \frac{N_{Ed}}{2.N_{f.Rd}})}{M_{eff.Rd}.(1 - \eta_4)} && \text{, if web not fully compressed} \\ &\eta_{1.f} = 0 && \text{, if web fully compressed} \\ &\mu = (\eta_{1.f} + 0{,}2)^{15} + 1 \end{aligned} \qquad (3)$$

2. Design methods to obtain the critical stresses

2.1. Investigated parameter range

The definition of the geometries that were considered in this analysis was made in such a way that accounted for a vast range of typical plate girders. A total of 80 cross-sections were selected using the following parameters:

- $\frac{h_w}{t_w} = [60, 80, 100, 120, 140, 160, 180, 200, 220, 240]$
- $h_w = 1000mm$ ▪ $b_{si} = 100mm$ ▪ $b_{ss} = 50mm$
- $\gamma = [25, 50, 75, 100]$ ▪ $\alpha = \frac{a}{h_w} = [1, 2]$

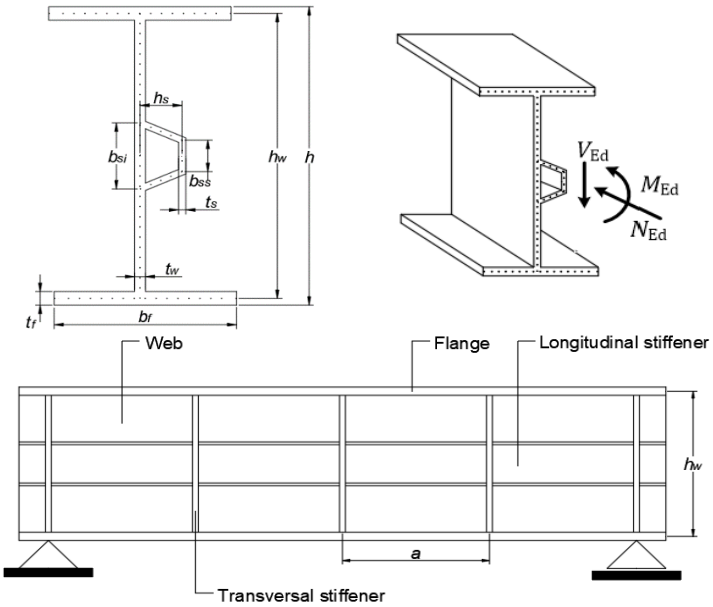

Figure 2: Design of S690 slender plate I-girders under combined shear, bending and compression

2.2. Torsional stiffness of the longitudinal stiffener ($\sigma_{cr.p}$, τ_{cr})

First, the torsional stiffness of the longitudinal stiffener needs to be assessed. Thus, 4 different models were developed to verify the need to consider, or not, the torsional stiffness of the longitudinal stiffener, something that should be neglected according to the standard EN 1993-1-5 [2]. In that regard, the critical stresses $\sigma_{cr.p}$, for the compression and bending moment, and τ_{cr}, for the shear stress, were obtained for each model, whereas everything else follows the EN 1993-1-5, particularly the calculation of the critical stresses $\sigma_{cr.loc}$ and $\sigma_{cr.c}$.

2.2.1. Model 1 – 1 General Shape considering θ

This first model intends to be as close as possible to reality, considering the torsional stiffness of the longitudinal stiffener. For this purpose, to quantify the critical stresses $\sigma_{cr.p}$ and τ_{cr}, it will be necessary to use the EBPlate [8] functionalities, an automatic numerical calculation software.

2.2.2. Model 2 – 2 General Shape neglecting θ

The analysis of this second model turns out to be the first attempt to remove the torsional stiffness from the longitudinal stiffener. It was decided to divide the trapezoidal closed section, which present high values of θ, in two open sections, where the values of torsional stiffness end up being limited (Figure 3). It should be noted that each one of these stiffeners must be modelled with half of the properties of the longitudinal stiffener and the adjacent parts of the plate, $\delta'' = \frac{\delta'}{2}$ and $\gamma'' = \frac{\gamma'}{2}$, ensuring that $\theta = 0$. The values of $\sigma_{cr.p}$ and τ_{cr} were obtained though EBP.

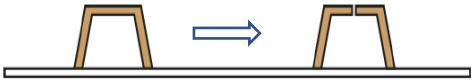

Figure 3: Study of the closed section longitudinal stiffener as two open section stiffeners

2.2.3. Model 3 - 1 General Shape neglecting θ

This model follows almost entirely what was presented for Model 1, with the difference that in the present case the relative torsional stiffness must me $\theta = 0$. It is intended to create a design model that is similar to what is presented in the EN 1993-1-5 [2], where the torsional stiffness is neglected. The longitudinal stiffener must be created with the properties established in Model 1, considering an adjacent part of the plate, γ' and δ'. The values of $\sigma_{cr.p}$ and τ_{cr} were obtained though EBPlate.

2.2.4. Model 4 – EN 1993-1-5

The last model is entirely based on the formulations presented in EN 1993-1-5, which means that the critical stresses $\sigma_{cr.p}$ and τ_{cr} were obtained through the EN 1993-1-5 formulas, neglecting the effect of the torsional stiffness of the longitudinal stiffener.

To have a solid and reliable basis for comparison, numerical models for all geometries were developed using finite element analysis software Abaqus [9], which are the comparison term between the different models.

3. Numerical model of non-linear analysis

3.1. Model assumptions

Several numerical models were built up using the multi-purpose code Abaqus-Python [9] interpreter and MATLAB [10] subroutines. The analysis is conducted using the Modified Riks Method [11] and include equivalent geometric imperfections and material non-linearity (GMNIA). Modified Riks Method is chosen as it allows to overcome the convergence problems associated with solving non-linear systems of equations, by using an iterative procedure of variation of the applied load. Still, some convergence problems were found in some models, leading to incorrect results, commonly known as back-tracking. For the number of plate elements, studies were carried out to find out which solution allows to reproduce the structural behaviour with enough accuracy, and it was concluded that considering a square panel with $\alpha = 1$, 30 quadrangular elements along the longitudinal edges attend the purpose of this investigation. For the boundary conditions, studies were carried out to understand which ones suited better this study, confirming that the longitudinally stiffened slender plates and I-girders should be designed with the four edges simply supported.

3.2. Material models

Following the von Mises criterion in the numerical calculation, the material model used behaves elastically until it reaches the yield stress $f_y = 690$ MPa, with a Young modulus equal to 210 GPa. Once the elastic properties of the material are fully utilized, a nominal hardening phase takes place until it reaches the ultimate resistance of the structure, f_u. The properties used to define the material model are listed in Table 1 and shown in Figure 4:

Table 1: Parameters used in the material model

E	E_{sh}	f_y	$f_{C1\varepsilon u}$	f_u	C_1
210 GPa	6,185 GPa	690 MPa	740 MPa	770 MPa	0,61
ε_y	ε_{sh}	$C_1\varepsilon_u$	$C_2\varepsilon_u$	ε_u	C_2
0,33%	3%	3,81%	4,29%	6,23%	0,69

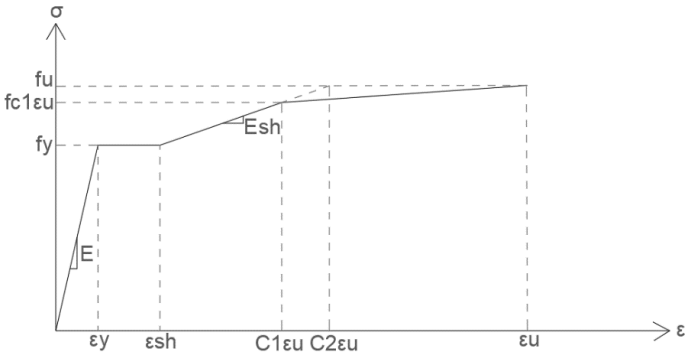

Figure 4: Stress-strain law used in the FEM model

3.3. Equivalent geometric imperfections

In slender plate elements the geometric and material imperfections must be accounted for the calculation of the structural strength, once the collapse is governed by plate buckling. In addition, there is also the contribution of residual stresses, associated with the differential thermal effects that take place during the processes of hot rolling or welding of the different plates. In that regard, it is essential to perform the modelling of the numerical models considering an equivalent geometric imperfection, as given in EN 1993-1-5 [2]. Thus, 3 different equivalent geometric imperfections were developed based on periodic functions, and a sensitivity analysis was carried out to determine which one should be used in the modelling of numerical models. For this purpose, a sample of 12 geometries was selected.

i. Equivalent geometric imperfection 1 (IMP 1)

This equivalent geometric imperfection is a global imperfection of the stiffened panel, defined by a sine function with an amplitude of $h_w/400$ (Figure 5):

- **IMP 1 +** $+sen \times \frac{h_w}{400}$
- **IMP 1 -** $-sen \times \frac{h_w}{400}$

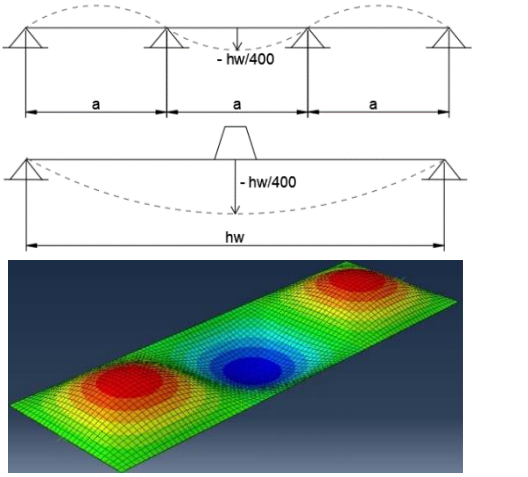

Figure 5: Equivalent geometric imperfection with negative amplitude (IMP 1 -)

ii. Equivalent geometric imperfection 2 (IMP 2)

The second one results from the crossing of two different forms of imperfections: a global imperfection of the stiffened panel defined by a sine function with an amplitude of $h_w/400$, coupled with a local imperfection of the sub-panels between the stiffener and the longitudinal edges, also defined by a sine function with an amplitude of $b_i/200$, symmetrical in relation to the longitudinal stiffener (Figure 6).

- **IMP 2 +** $+\frac{b_i}{200} \times w_{buckling}^{simétrico} + sen \times \frac{h_w}{400}$
- **IMP 2 -** $-\frac{b_i}{200} \times w_{buckling}^{simétrico} - sen \times \frac{h_w}{400}$

iii. Equivalent geometric imperfection 3 (IMP 3)

Finally, the third equivalent geometric imperfection is based on the previous one, combining a global imperfection with a local one. However, in this case we assume that the local imperfection is asymmetrical in relation to the longitudinal stiffener (Figure 7).

- **IMP 3 +** $+\frac{b_i}{200} \times w_{buckling}^{anti-simétrico} + sen \times \frac{h_w}{400}$
- **IMP 3 -** $+\frac{b_i}{200} \times w_{buckling}^{anti-simétrico} - sen \times \frac{h_w}{400}$

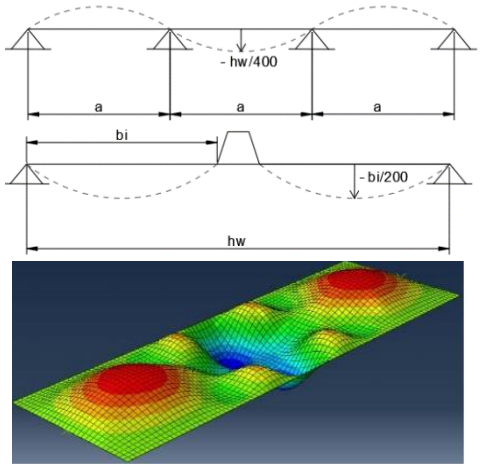

Figure 6: Equivalent geometric imperfection with negative amplitude (IMP 2 -)

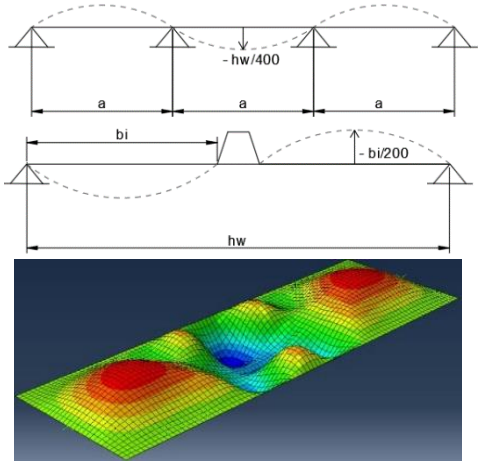

Figure 7: Equivalent geometric imperfection with negative amplitude (IMP 3 -)

3.4. Sensitivity to equivalent geometric imperfections

For this purpose, the ultimate resistances of the geometries were obtained using the numerical analysis software Abaqus [9] when subjected to compression, bending moment and transverse stresses, individually, where it can be pointed out that the imperfection 2 with negative amplitude is the one that generally presents the minimum resistances for each geometry. The results obtained for the ultimate resistances of the different geometries subjected to compression, bending moment and transverse stress, numbered from 1 to 12, are presented in Figure 8, where the values are normalized to the ultimate resistances that were verified for panels with IMP 2 with negative amplitude.

4. Numerical results for N, M, V stresses

4.1. Torsional stiffness of the longitudinal stiffener ($\sigma_{cr.loc}$)

A brief analysis on the consideration of the torsional stiffness of the longitudinal stiffener was carried out along with the calculation of the critical stress $\sigma_{cr.loc}$. For this purpose, the ultimate resistance of the 80 geometries subjected to pure compression were calculated following the standard EN 1993-1-5 [2] in two different ways, considering a variation of k_σ: $k_\sigma = 4$, corresponding to a situation in which the torsional

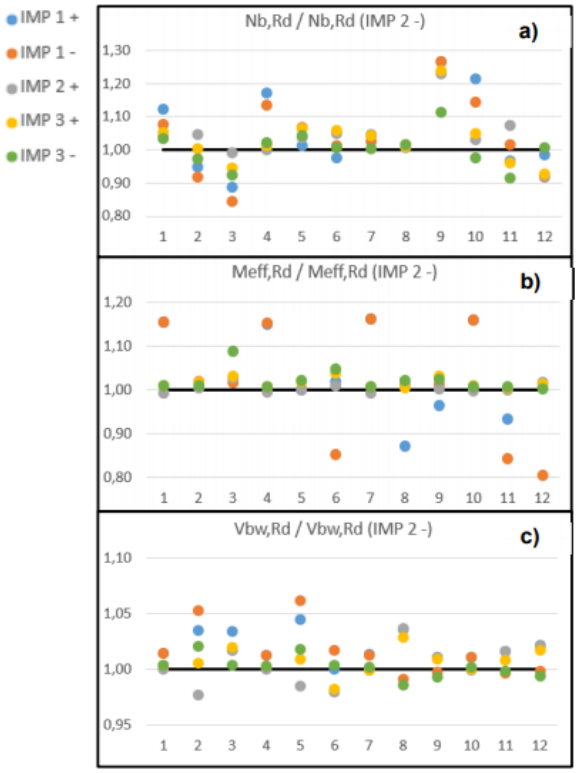

Figure 8: Sensitivity analysis to axial stress [a)], bending moment [b)] and transverse stress [c)]

stiffness is neglected, and $k_\sigma = 5{,}5$, where the torsional stiffness of the stiffener is considered. It was concluded that neglecting this stiffness is always a decision that is clearly on the safety side (Figure 9). The ultimate resistances to axial compression are normalized to the ultimate resistances obtained with $k_\sigma = 4$.

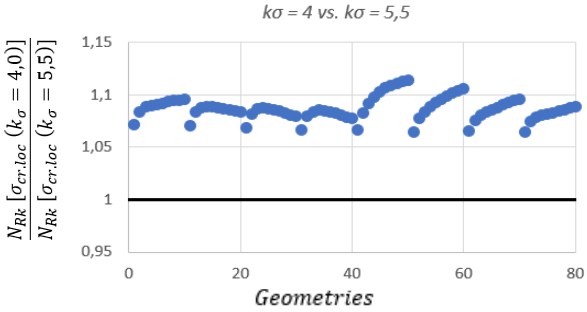

Figure 9: Torsional stiffness study with $k_\sigma = 4{,}0$ vs. $k_\sigma = 5{,}5$

4.2. Analysis of the different numerical models

The analysis is based on the comparison between the different design models presented in § 2 and the numerical models developed for each geometry of longitudinally stiffened slender plates, subjected to the stresses N, M, and V, acting separately. It is important to note that the results obtained were normalized: the axial force was normalized to the plastic axial stress, N_{pl}, the bending moment to the effective bending moment to the outside plane direction, $M_{eff.y}$, and the transverse force to the plastic transverse stress of the web, $V_{pl,w}$.

Table 2: $N_{b.FEM}/N_{b.Rd}$, $M_{eff,y,FEM}/M_{eff,y.Rd}$, $V_{bw,FEM}/V_{bw,Rd}$

	avg	std	avg	std
$N_{b,FEM}/N_{b,Rd}$	$\alpha = 1$		$\alpha = 2$	
MODEL 1	1,139	4,7%	1,152	12,3%
MODEL 2	1,140	4,8%	1,156	12,2%
MODEL 3	1,140	4,8%	1,160	12,1%
MODEL 4	1,153	5,3%	1,209	
$M_{eff.y.FEM}/M_{eff.y.Rd}$	$\alpha = 1$		$\alpha = 2$	
MODEL 1	1,422	14,6%	1,390	12,4%
MODEL 2	1,423	14,6%	1,394	12,5%
MODEL 3	1,422	14,6%	1,391	12,4%
MODEL 4	1,423	14,6%	1,398	12,4%
$V_{bw.FEM}/V_{bw.Rd}$	$\alpha = 1$		$\alpha = 2$	
MODEL 1	0,980	3,4%	0,976	7,4%
MODEL 2	0,992	3,5%	1,055	7,9%
MODEL 3	1,056	4,9%	1,106	8,9%
MODEL 4	1,162	8,2%	1,236	11,5%

Conclusions on the $N_{b,FEM}/N_{b,Rd}$ analysis:

- There is a similarity of the average and standard deviation values obtained for the various design models both for $\alpha = 1$ or $\alpha = 2$.
- There is practically no difference between the models that consider the effect of the torsional stiffness of the stiffener and the ones that do not. That is because these structures were designed exclusively with one longitudinal stiffener, being certain that the differences between the various models would be more conclusive with 2 or 3 stiffeners.
- Model 4 – EN 1993-1-5 is associated with a very high average compared to the other calculation models, which indicates that the current formulations to obtain the critical stress $\sigma_{cr.p}$ are conservative, especially for higher aspect ratios.

Conclusions on the $M_{eff,y,FEM}/M_{eff,y.Rd}$ analysis:

- It´s clear that for the case of longitudinally stiffened slender plates subjected to bending moments, the calculation models appear to be very conservative and with great dispersion of results.
- The high averages obtained for both $\alpha = 1$ and $\alpha = 2$ are due to the consideration of the yielding of the tension sub-panel in the calculation of $M_{eff,y.FEM}$ through the automatic numerical calculation software, something that is not estimated in $M_{eff,y.Rd}$ through the different design models in evaluation based on EN 1993-1-5 [2] (Figure 10).
- The buckling modes do not involve the torsional stiffness of the stiffener since the plate naturally does not tend to rotate there, but on the longitudinal edges. In that regard, there is practically no difference between the models that consider the effect of the torsional stiffness of the stiffener and the ones who that do not. However, studies with 2 or 3 stiffeners surely would be more conclusive.

Conclusions on the $V_{bw,FEM}/V_{bw,Rd}$ analysis:

- It is proven why the consideration of the torsional stiffness of the longitudinal stiffener should be neglected in the structural calculation present in the standard EN 1993-1-5, once the first model, which considers this effect, exhibits numerous cases where $V_{bw,FEM}/V_{bw,Rd} < 0{,}90$, either for $\alpha = 1$ or $\alpha = 2$.
- Despite Model 3 presents a number of cases violating the condition $V_{bw,FEM}/V_{bw,Rd} < 1{,}0$ higher than for Model 4, it appears to be composed by a design method much more economic and reliable, once it's associated with lower values of averages and standard deviations.

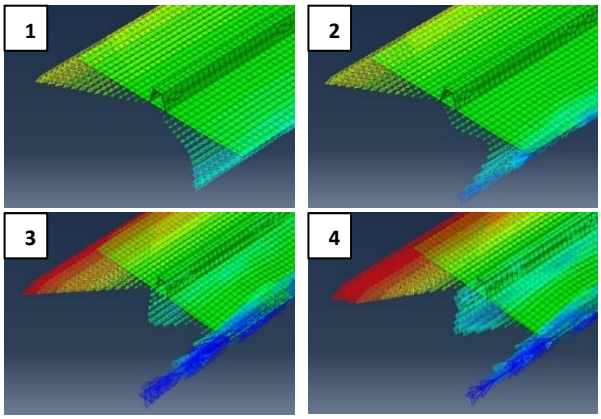

Figure 10: Effect of the longitudinal stiffener on the evolution of compression stresses along a longitudinally stiffened slender plate subjected to a bending moment in the transverse direction

From the summary analysis to the results obtained, it can be pointed out that Model 4 is a very conservative design method, being always associated with very high values of averages and standard deviations. However, it proves to be well structured and calibrated for the calculation of the critical stress $\sigma_{cr.p}$, both for the axial compression and bending moment. Still, a great difference was obtained for the calculation of the critical stress τ_{cr}. Thus, Model 3 is the one that appears to be the best choice to continue this investigation, since it is a safe and economical design method, and not so on the safe side as the formulas proposed by the EN 1993-1-5 [2].

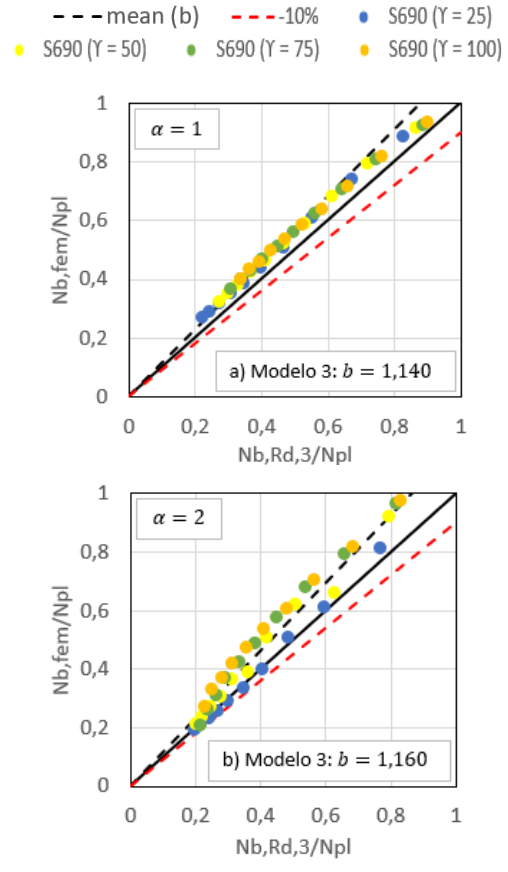

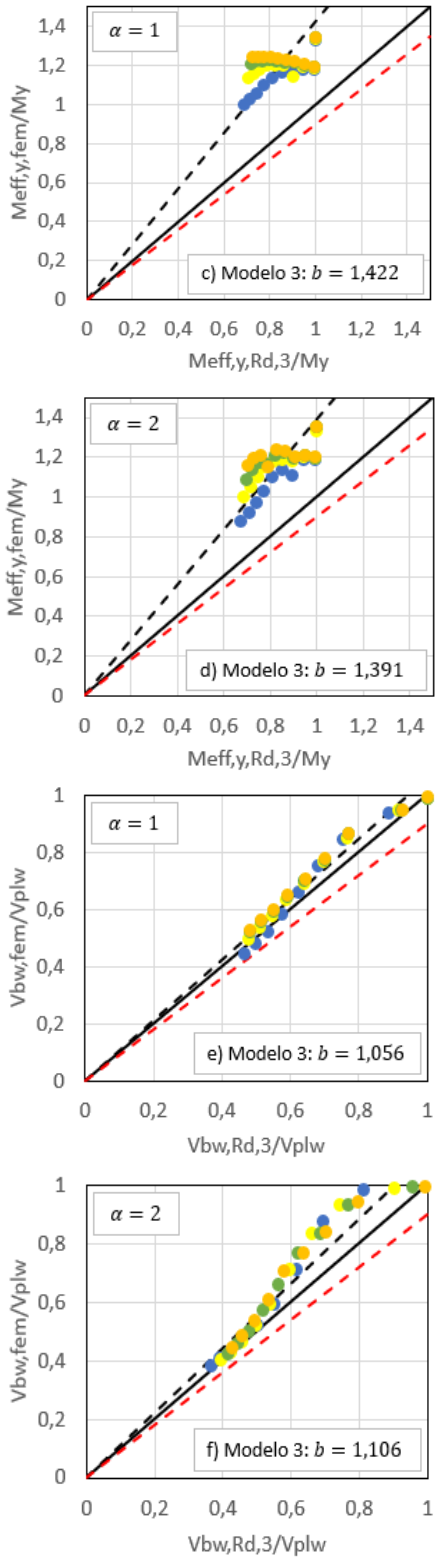

Figure 11: Graphics of Model 3: $N_{b.FEM}/N_{b.Rd}$ [a) and b)], $M_{eff.y.FEM}/M_{eff.y.Rd}$ [c) and d)], $V_{bw.FEM}/V_{bw.Rd}$ [e) and f)]

4.3. Influence of the flanges on the calculation of the $V_{b.Rd}$

Following Model 3, the next 20 geometries of longitudinally stiffened slender plates were considered with the area ratios $A_f/A_w = [0; 0{,}25; 0{,}50; 1]$:

- ID1_ID5: $\frac{h_w}{t_w}$ between 80 and 240 with $\gamma = 25$ and $\alpha = 1$
- ID6_ID10: $\frac{h_w}{t_w}$ between 80 and 240 with $\gamma = 50$ and $\alpha = 1$
- ID11_ID15: $\frac{h_w}{t_w}$ between 80 and 240 with $\gamma = 25$ and $\alpha = 2$
- ID16_ID20: $\frac{h_w}{t_w}$ between 80 and 240 with $\gamma = 50$ and $\alpha = 2$

Attending on Figure 12, there is a clear influence that the contribution of the resistance of the flanges, $V_{bf,Rd}$, has in the utimate resistance of the profile to transverse stresses, $V_{b.Rd}$. It appears that, while for webs with a high slenderness the dispersion of results is considerably reduced, with a good correlation between the ultimate resistances obtained through the formulations of the EN 1993-1-5 [2] and the values obtained trough automatic numerical calculation programs based on finite elements, for webs with an intermediate slenderness it is observed a tendency for the ocurrence of greater dispersions. That's due to the fact that, in a first instance, EN 1993-1-5 underestimates the value of the $V_{bf,Rd}$, whereas for stronger flanges, with a larger area, it seems to overestimate this value. Thus, for this reason, considering large areas for the flanges may compromise the structural security of the element, especially for intermediate slenderness webs, something that had already been concluded by Jáger and Kövesdi [5, 6].

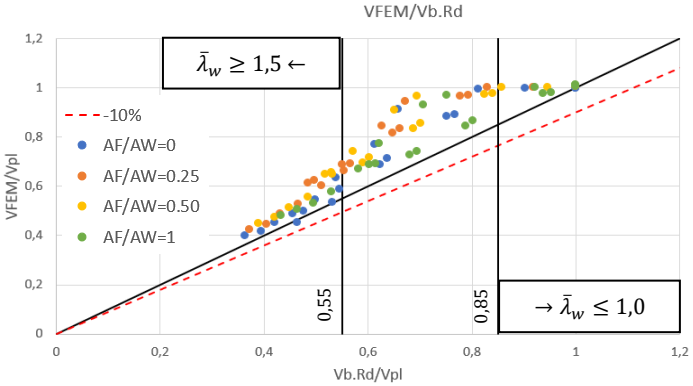

Figure 12: Influence of the flanges on the calculation of $V_{b.Rd}$

5. Study of the N-M-V interaction

5.1. N-M-V interaction following the new Biscaya proposal

Consider the following relations between the applied and resistance forces, accounting for the eccentricity due to local web buckling, e_N:

- $\eta_{1.M} = \frac{M_{Ed}+N_{Ed}.e_N}{M_{eff.Rd}}$
- $\bar{\eta}_3 = \frac{V_{Ed}}{V_{bw,Rd}}$
- $\eta_{1.N} = \frac{N_{Ed}}{N_{eff.Rd}}$ (4)

which must be lower or equal to the unit. For an axial force $N_{Ed} > 0$ and $\bar{\eta}_3 \geq 0{,}5k$, it must be ensured that:

$$\eta_{1.M} + \eta_{1.N} + \left(1 - \frac{M_{\mathrm{f,N,Rd}}}{M_{\mathrm{eff,Rd}}} - \eta_{1.N}\right)\left(\frac{2\bar{\eta}_3}{k} - 1\right)^{\mu} \leq 1 \quad , \eta_{1.M} \geq \frac{M_{\mathrm{f,N,Rd}}}{M_{\mathrm{eff,Rd}}} \qquad (5)$$

$$\bar{\eta}_3 \leq k + \frac{V_{\mathrm{bf,N,Rd}}}{V_{\mathrm{bw,Rd}}}\left[1 - \left(\frac{M_{\mathrm{Ed}}}{M_{\mathrm{f,N,Rd}}}\right)^2\right] \quad , \eta_{1.M} < \frac{M_{\mathrm{f,N,Rd}}}{M_{\mathrm{eff,Rd}}} \qquad (6)$$

with k to be defined as follows:

$$k \begin{cases} = 1 & , \eta_{1.N} \le \left(\frac{V_{b,Rd}}{V_{bw,Rd}} - 1\right)/i \\ = \frac{V_{b,Rd}}{V_{bw,Rd}} - i \cdot \eta_{1.N} & , \left(\frac{V_{b,Rd}}{V_{bw,Rd}} - 1\right)/i < \eta_{1.N} \le \frac{N_{f,Rd}}{N_{eff,Rd}} \\ = \sqrt{\frac{1-\eta_{1.N}{}^{\beta}}{\xi}} & , \eta_{1.N} > \frac{N_{f,Rd}}{N_{eff,Rd}} \end{cases} \quad (7)$$

where:

- $M_{f,N,Rd} = M_{f,Rd}(1 - \frac{N_{Ed}}{N_{f.Rd}})$, ensuring that $N_{Ed} \le N_{f.Rd}$. Otherwise, it must be considered $M_{f,N,Rd} = 0$.
- $M_{eff,Rd} = W_{eff} \times f_y$
- $N_{f,Rd} = (A_{f1} + A_{f2}) \times f_{yf}$
- $V_{bw,Rd}$ and $V_{bf,Rd}$ apply formulas (7.1), (7.2) and (7.7 with $M_{Ed} = 0$) presented in the European standard, without the partial factor γ_{M1}.
- $V_{bf,N,Rd} = V_{b,Rd}(1 - i.\eta_{1.N}) - V_{bw,Rd} \ge 0$
- $\mu = \left(\frac{M_{f,N,Rd}}{M_{eff,Rd}} + 0{,}2\right)^{15} + 1$
- $i = \frac{1}{2} - e^{-\bar{\lambda}} \ge 0$
- $\beta = 1 + \frac{1}{\bar{\lambda}^2} \le 2$
- $\xi = \frac{1-(\frac{N_{f,Rd}}{N_{eff.Rd}})^{\beta}}{(1-i.\frac{N_{f,Rd}}{N_{eff.Rd}})^2}$

For longitudinally stiffened slender plates and I-girders,

$$\bar{\lambda} = máx(\bar{\lambda}_{loc} = \sqrt{\frac{f_y}{\sigma_{cr.loc}}};\ \bar{\lambda}_p = \sqrt{\frac{\beta_{A.c}\, f_y}{\sigma_{cr.p}}})$$

whereas for unstiffened ones it must be simply considered $\bar{\lambda} = \bar{\lambda}_p$. In that regard, it is worth noting that these values are defined for pure compression once this part of the interaction was defined in the N-V plane. In addition, studies were made in order to validate this proposition, where it could be pointed out that, despite for cases with only one longitudinal stiffener positioned at half height of the web, $h_w/2$, the parameter that best suits $\bar{\lambda}$ is $\bar{\lambda}_{loc}$, with rare exceptions, H. Afonso [12], studies conducted by Biscaya [1] for slender plates and I-girders with 2 and 3 longitudinal stiffeners showed that the best definition for the parameter $\bar{\lambda}$ is the maximum value of $\bar{\lambda}_{loc}$ and $\bar{\lambda}_p$, both obtained for pure compression, as described in the final N-M-V interaction proposal.

5.2. Investigated parameter range

The definition of the geometries that were considered in this analysis was made in such a way that accounted for a vast range of typical plate girders. A total of 20 cross-sections were selected using the following parameters:

- $\frac{h_w}{t_w} = [80, 120, 160, 200, 240]$
- $\gamma = [25, 50]$
- $\alpha = [1, 2]$

Thus, the 20 geometries to be used in this final study were defined as follows in § 4.3. It is worth noting that new geometries were not created here, the initial number of 80 is only reduced to 20. Finally, it is essential to explain how the flanges were introduced in the investigation. To be able to assess the contribution of the flanges to increase the structural stability of the slender plates, 4 values were defined for the ratio of areas $A_f/A_w = [0; 0{,}25; 0{,}50; 1]$, with $b_f = \sqrt{8 \times A_f}$ and $t_f = \frac{b_f}{8}$.

5.3. N-M-V interaction surface

It is now interesting to explain how the investigation was set up in regard to the modelling of the N-M-V interaction surface. Briefly, the interaction surface will follow a spherical coordinates system, as shown in Figure 13, where the coordinates are obtained trough the following equations:

- $\frac{N_{FEM}}{N_{Model\_3}} = LPF \times \cos\theta_1 \times \cos\theta_2$
- $\frac{M_{FEM}}{M_{Model\_3}} = LPF \times \text{sen}\,\theta_1 \times \cos\theta_2$
- $\frac{V_{FEM}}{V_{Model\_3}} = LPF \times \sin\theta_2$

with θ_1 and θ_2 varying between 0º and 90º with intervals of 15º.

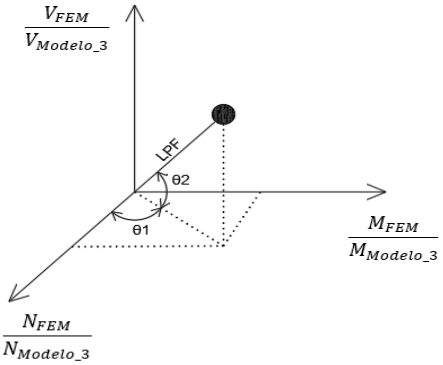

Figure 13: Illustration of the spherical coordinates system to be used

The plotting of the N-M-V interaction points can be seen as the creation of 7 curved surfaces, each one consisting on 7 interaction points. Figure 14 helps to understand what is intended to explain here, where:

$$R = \sqrt{(\frac{N_{Ed}}{N_{eff.Rk}})^2 + (\frac{M_{Ed}}{M_{eff.Rk}})^2 + (\frac{V_{Ed}}{V_{bw.Rk}})^2}.$$

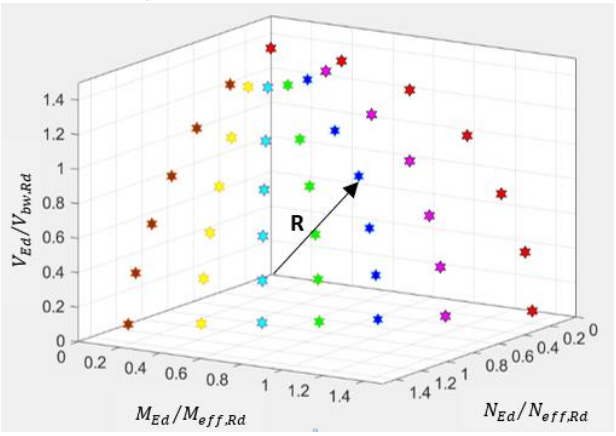

Figure 14: N-M-V interaction points

Finally, it is worth to make some considerations regarding the non-convergence of results derived from problems associated with solving non-linear equations systems, as seen in §3. Indeed, these situations did hapen in the course of the investigation. However, they were properly identified and discarted from the statistical analysis, once they do not guarantee the reliability deserved for this study. Though, despite the fact that these convergence problems occured, it should be noted that they represent only 1,4% of the total sample, that is from all points of the N-M-V interaction of all the 20 geometries under study, and accounting for the different A_f/A_w ratios under analysis, so they will not have a significant impact on the final conclusions of this investigation at all.

5.4. N-M-V interaction surface analysis

Table 3: N-M-V interaction according to the standard EN 1993-1-5 [2] and the Biscaya proposal [1]

$\frac{R_{FEM}}{R_{PROPOSAL}}$	avg	std	$N_{cases} < 1,0$	$N_{cases} < 0,9$	$Mín.$	$Máx.$
	$A_f/A_w = 0$					
EN 1993-1-5	1,192	13,6%	6,3%	0,2%	0,890	1,637
PROPOSAL	1,200	12,9%	2,9%	0%	0,956	1,637
	$A_f/A_w = 0,25$					
EN 1993-1-5	1,214	9,8%	1%	0%	0,908	1,550
PROPOSAL	1,190	8,3%	0,4%	0%	0,978	1,405
	$A_f/A_w = 0,50$					
EN 1993-1-5	1,203	10,2%	0,3%	0%	0,988	1,600
PROPOSAL	1,158	7,5%	0,7%	0%	0,968	1,393
	$A_f/A_w = 1$					
EN 1993-1-5	1,165	10,5%	0,3%	0%	0,996	1,517
PROPOSAL	1,102	6,9%	5,4%	0%	0,930	1,314

Conclusions on the $R_{FEM}/R_{PROPOSAL}$ analysis:

- The new Biscaya proposal [1] gives better results of the real N-M-V interaction resistance than the current version of EN 1993-1-5 [2], as the differences between the averages and the standard deviations are considerable.
- It can be pointed out that the new proposal is less conservative than the EN 1993-1-5 formulas: it is observed that the proposal returns significantly lower values of averages for all cases, except for $A_f/A_w = 0$, which can be explained by the poor calibration of slender plates by the EN 1993-1-5. However, since the proposal does not return any situations where $R_{FEM}/R_{PROPOSAL} < 0{,}9$ and, in addition, returns a small number of cases in which $R_{FEM}/R_{PROPOSTA} < 1$, still having a lower value for the standard deviation, it can be assumed that the new proposal is more appropriate for the N-M-V interaction assessment.
- The new calculation method seems to be more reliable, once it returns lower values for the standard deviations, being transversal to the application of the flanges, ensuring a smaller dispersion of results and consequently a greater reliability of this equations.
- It is confirmed that the contribution of $V_{bf,Rd}$ in the calcultaion of $V_{b.Rd}$ has a negative effect on the N-M-V interaction resistance, having an impact on the final results. It can be pointed out that firstly the values of the averages increase, and then show a successively decreasing trend, confirming what was concluded by Jáger and Kövesdi [5, 6], regarding the erroneous consideration of the contribution of the flange shear resistance due to the bad calibration of the value of $V_{bf,Rd}$ by means of parameter c (distance between the plastic hinges). This subject needs further investigation.

The final graphs associated with the results from Table 3 are presented in Figures 15 and 16, which show the behaviour observed for the different A_f/A_w ratios.

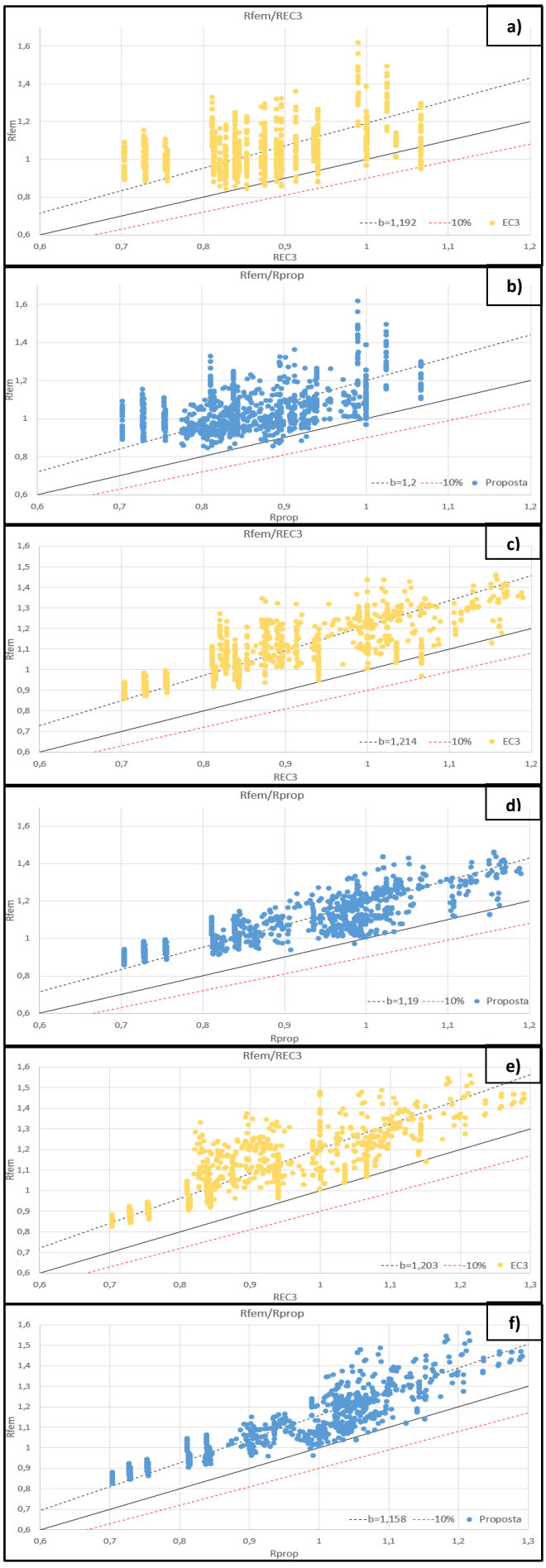

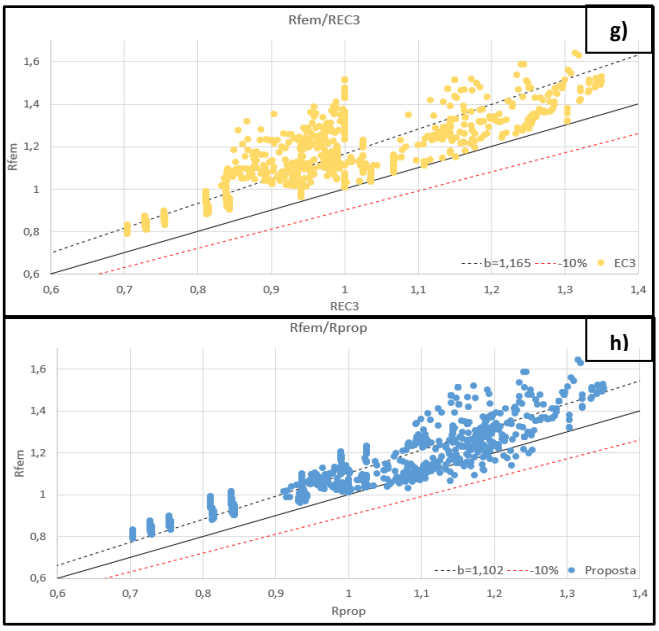

Figure 15: R_{FEM}/R_{EC3} and $R_{FEM}/R_{PROPOSAL}$ for the ratios: $A_f/A_w = 0$ [a) and b)], $A_f/A_w = 0{,}25$ [c) and d)], $A_f/A_w = 0{,}50$ [e) and f)], $A_f/A_w = 1$ [(g) and h))]

There follows a presentation and analysis of some N-M-V interaction surfaces chosen so that it is possible to identify and assess the impact and relevance that some factors have in the design of longitudinally stiffened slender plates and I-girders: the slenderness of the plate, h_w/t_w, the flexural stiffness of the longitudinal stiffener, γ, and the aspect ratio to consider, α, considering $A_f/A_w = 0{,}50$, always based on the new Biscaya proposal [1].

ID 1 // $\gamma = 25$ // $\alpha = 1$ // $\frac{h_w}{t_w} = 80$ // $\frac{A_f}{A_w} = 0{,}50$

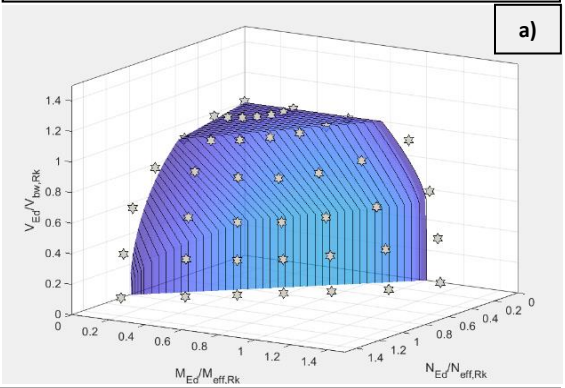

ID 5 // $\gamma = 25$ // $\alpha = 1$ // $\frac{h_w}{t_w} = 240$ // $\frac{A_f}{A_w} = 0{,}50$

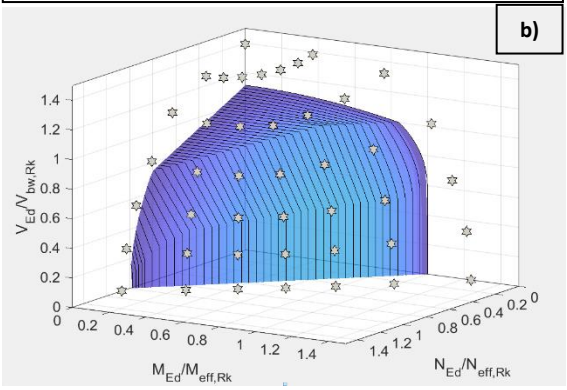

ID 3 // $\gamma = 25$ // $\alpha = 1$ // $\frac{h_w}{t_w} = 160$ // $\frac{A_f}{A_w} = 0{,}50$

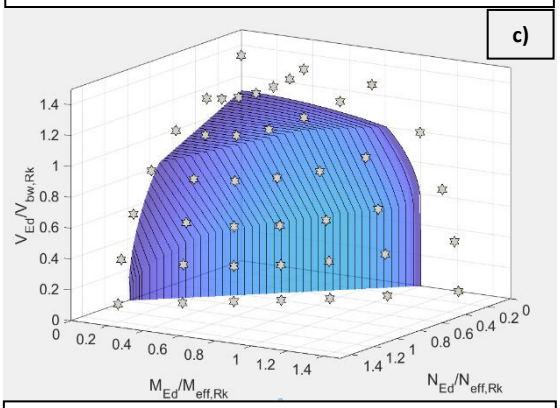

ID 8 // $\gamma = 50$ // $\alpha = 1$ // $\frac{h_w}{t_w} = 160$ // $\frac{A_f}{A_w} = 0{,}50$

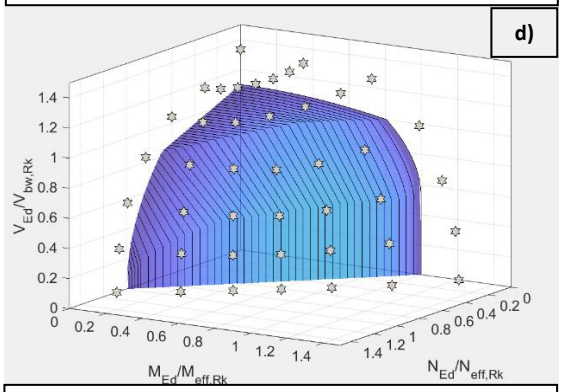

ID 7 // $\gamma = 50$ // $\alpha = 1$ // $\frac{h_w}{t_w} = 120$ // $\frac{A_f}{A_w} = 0{,}50$

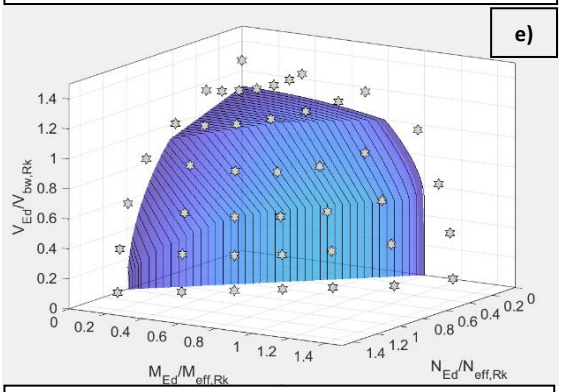

ID 17 // $\gamma = 50$ // $\alpha = 2$ // $\frac{h_w}{t_w} = 120$ // $\frac{A_f}{A_w} = 0{,}50$

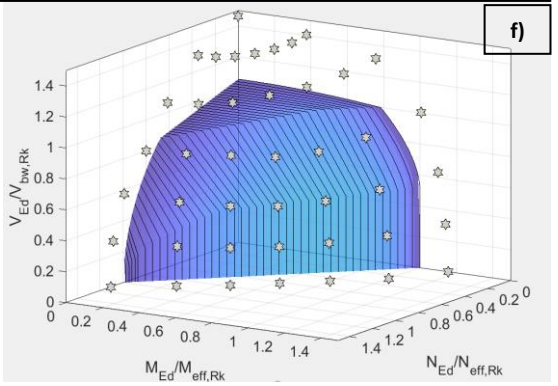

Figure 16: Effect of the slenderness of the plate h_w/t_w [a) and b)], the flexural stiffness of the longitudinal stiffener γ [c) and d)] and the aspect ratio α [e) and f)] on the N-M-V interaction surface

Conclusions on the effect of the slenderness of the plate (h_w/t_w):

- There is clearly a notorious difference between considering, or not, slender plates. It can be pointed out that while for lower values of h_w/t_w there is a consistency between the N-M-V surface and the interaction points obtained through automatic numerical calculation programs of finite elements, which appears to be trasversal to the A_f/A_w ratios under study, for very slender plates the same does not happen, once there is a large resistance reserve in relation to the numerical models.
- It is evident that there is a large increase of the resistance reserve when the flanges are introduced in the problem, with a sucessively reduction of it when the geometry of these elements is increased, as mentioned and discussed before.

Conclusions on the effect of the flexural stiffness of the longitudinal stiffener (γ):

- It is noted that there are no major differences when analysing slender plates and I-girders with $\gamma = [25; 50]$, due to the fact that this investigation only considers weak longitudinal stiffeners, which ends up conditioning the occurrence of notable dissimilarities. However, there is a slight increse of the resistance reserve to higher values of γ, as expected.
- It can be confirmed once again the effect that the influence of the flanges appear to have on the development of the N-M-V interaction surface: wheras for intermediate A_f/A_w ratios there is a large reserve of the new proposal in relation to the points obtained according to the finite element numercial models, it tends to decrease as this quocient increases.

Conclusions on the effect of the aspect ratio (α):

- For both aspect ratios aspect ratios $\alpha = 1$ and $\alpha = 2$, the resistances obtained using the formulation from prEN 1993-1-5 [13] are low when compared to the numerical resistances obtained, independently of the A_f/A_w adopted. This margin is increased for long web panels with $\alpha = 2$
- The negative effect that the contribution of $V_{bf.Rd}$ has on the design of slender I-girders is confirmed, with notable tendency to obtain results outside the safety zone for higher A_f/A_w ratios and small α values, contributing to a lower resistance reserve of the N-M-V interaction surface in relation to the numerical interaction points.

6. Main conclusions

From studies on the N-V and N-M-V interaction behaviour of longitudinally stiffened I-girders with slender webs, the following main conclusions are drawn:

- The question of whether to consider, or not, the torsional stiffness of the closed section longitudinal stiffener in the design of these profiles was analysed, where the critical stresses $\sigma_{cr.loc}$, $\sigma_{cr.p}$, and τ_{cr} were analysed:

1. $\sigma_{cr.loc}$ (Figure 9): using $k_\sigma = 4$ in the calculation of $\sigma_{cr.loc}$, which is the same as neglecting this rigidity, the results will always be on the safety side, confirming the note present on the European standard EN 1993-1-5 [2] in that regard.
2. $\sigma_{cr.p}$ and τ_{cr}: 4 different models were developed, all based on the formulation present in the EN 1993-1-5, where the only difference is based on how these critical stresses were obtained: for the first 3 models through EBPlate [8], with and without considering the torsional stiffness of the longitudinal stiffener, whereas for Model 4, all formulations of the prEN 1993-1-5 [13] were followed.

2.1. It is concluded that Model 4 – EN 1993-1-5 is very conservative when compared to the other models, showing to be a methodology that is well calibrated for the calculation of the critical stress $\sigma_{cr.p}$, but not for the calculation of τ_{cr}.

2.2. It is also concluded that EN 1993-1-5 [2] does not consider the redistribution of stresses that the longitudinal stiffener provides when the slender plate is subjected to bending moments (Figure 10), giving a large resistance reserve, contributing to an excessive conservatism.

2.3. Model 3 is the one that provides the best results, as it is a safe and economical calculation methodology, for the design of longitudinally stiffened slender plates and I-girders.

- Regarding Biscaya new interaction proposal [1], it was analysed what value of $\bar{\lambda}$ should appear on it. It was concluded that, despite for the case of a longitudinal stiffener at mid height of the web, it should be assumed $\bar{\lambda} = \bar{\lambda}_{loc}$, with rare exceptions, further studies with 2 and 3 stiffeners have shown that $\bar{\lambda}$ should be given by:

$$\bar{\lambda} = máx\ (\bar{\lambda}_{loc} = \sqrt{\frac{f_y}{\sigma_{cr.loc}}};\ \bar{\lambda}_p = \sqrt{\frac{\beta_{A.c}\ f_y}{\sigma_{cr.p}}})$$

  both evaluated for pure compression.

- Comparing the data collected using the interaction equations suggested by the European standard and the new Biscaya proposal, the new N-M-V interaction equations prove to be more reliable from the point of view of the non-dispersion of results, being also more economical due to their lower conservatism. In addition, it is confirmed that it is a calculation method transversal to the use, or not, of longitudinal stiffeners, one of the main aims of this investigation, validating the initial premise.
- Common to all these analyses are undoubtedly the influence of the contribution of $V_{bf.Rd}$ on the design of these structures. In Figure 12, it is clearly identified the effect that the contribution of $V_{bf.Rd}$ has on the ultimate resistance $V_{b.Rd}$ of the profile, with direct implications on the N-M-V interaction results. This is essentially due to the fact that, in a first instance, EN 1993-1-5 underestimates the value of $V_{bf.Rd}$, whereas for more strong flanges, this parameter is overestimated, resulting on higher resistances than the ones obtained by the corresponding numerical models.

References

[1] A. Biscaya – *Buckling resistance of steel plated girders considering M-V interaction with high compression forces*, Instituto Superior Técnico, 2021, (in discussion).

[2] EN 1993-1-5 – *Eurocode 3 – Design of Steel Structures* – Part 1-5: Plated Structural elements, CEN, 2006.

[3] F. Sinur – *Behaviour of longitudinally stiffened plate girders subjected to bending-shear interaction*, University of Ljubljana, PhD Thesis, 2011.

[4] F. Sinur; D. Beg – *Moment-shear interaction of stiffened plate girders – Numerical study and reliability analysis*, J. Constr. Steel Res. 88, pags. 231-243, 2013.

[5] B. Jáger; B. Kövesdi; L. Dunai – *I-girders with unstiffened slender webs subjected by bending and shear interaction*, J. Constr. Steel Res. 131, 2017.

[6] B. Jáger; B. Kövesdi; L. Dunai – *Bending and shear buckling interaction behaviour of I-girders with longitudinally stiffened webs*, J. Constr. Steel Res. 145, 2018.

[7] A. Biscaya; J.J.O. Pedro; U. Kuhlmann – *Ultimate Strength of Slender Plate Girders under combined Shear, Bending and Compression*, Eurosteel, Sheffield, 2020.

[8] EBPlate, “Elastic Buckling of Plates”, Software Developed by CTICM in the Frame of the ComBri Project, RFCS Contract n RFS-CR-03018, 2006.

[9] SIMULIA, *Abaqus Scripting User´s Manual. Dassault Systems*, 2011.

[10] Matlab, *Matlab R2018*. MathWorks, 2018.

[11] B. G. Falzon; M. H. Aliabadi – *BUCKLING AND POSTBUCKLING STRUCTURES, Experimental, Analytical and Numerical Studies*, Computational and Experimental Methods in Structures – vol. 1, Imperial College Press, London, 2008.

[12] H. Afonso – *Dimensionamento de Vigas de Secção Soldada com Aço S690 sujeitas a Esforços Combinados de Flexão, Corte e Compressão*, Instituto Superior Técnico, 2021.

[13] prEN 1993-1-5 – *Eurocode 3 – Design of Steel Structures* – Part 1-5: Plated Structural elements, CEN, 2020.